Identifying the Lipid–Protein Interface of the *Torpedo* Nicotinic Acetylcholine Receptor: Secondary Structure Implications†

Michael P. Blanton and Jonathan B. Cohen*

Department of Neurobiology, Harvard Medical School, 220 Longwood Avenue, Boston, Massachusetts 02115

Received November 9, 1993; Revised Manuscript Received January 4, 1994®

ABSTRACT: To identify amino acid residues of the *Torpedo* nicotinic acetylcholine receptor (AchR) interacting with membrane lipid, we have used the photoactivatable, hydrophobic probe 3-trifluoromethyl-3-(*m*-[^{125}I]-iodophenyl)diazirine ([^{125}I]TID). The pattern of [^{125}I]TID incorporation into the M3 and M4 hydrophobic segments of each subunit was the same both in the presence and absence of the agonist carbamoylcholine and in the presence of an excess of nonradioactive TID, consistent with nonspecific photoincorporation from the lipid–protein interface. [^{125}I]TID reacted with five residues in α-M4 [Blanton, M. P., & Cohen, J. B. (1992) *Biochemistry 31,* 3738–3750] but with only two or three residues in M4 segments of β-, γ-, and δ-subunits. In δ-M3, [^{125}I]TID reacted with Met-293, Ser-297, Gly-301, Val-304, and Asn-305 as well as with Ile-288 preceding M3. Residues at corresponding positions were labeled in β-M3 (Met-285, Ile-289, Phe-293) and in γ-M3 (Phe-292, Leu-296, Met-299, and Asn-300) as well as γ-Ile-283. Within α-M3, Phe-284 and Ser-287 were labeled. The periodicity of labeled residues provides the first direct evidence that M3 as well as M4 segments of each subunit are organized as transmembrane α-helices each with substantial contact with lipid. In addition, in α-M1 [^{125}I]TID reacted nonspecifically with Cys-222, Leu-223, Phe-227, and Leu-228, a pattern of incorporation inconsistent with the labeling pattern expected either for a "face" of an α-helix or a β-sheet.

The nicotinic acetylcholine receptor (AchR)[1] from *Torpedo* electric organ is the best characterized member of a family of ligand-gated ion channels which includes the GABA receptor, the glycine receptor, and the 5HT-3 (serotonin) receptor. The AchR is composed of four homologous, transmembrane subunits in a stoichiometry of $\alpha_2,\beta,\gamma,\delta$ (Reynolds & Karlin, 1978; Raftery et al., 1980) which associate about a central axis to form a cation-selective channel [for recent reviews, see Stroud et al. (1990), Changeux et al. (1992), and Karlin (1991, 1993)].

Each subunit contains four hydrophobic segments 20–30 amino acids in length, referred to as M1–M4, that were proposed to be membrane-spanning α-helices (Noda et al., 1982, 1983a,b; Claudio et al., 1983). While there is strong evidence that these regions are in fact transmembrane [reviewed in Karlin (1991)], there is limited information available about their secondary structure or disposition relative to lipid or to the central axis of the AchR. The most information is available about the M2 regions for which results of both photoaffinity labeling studies with noncompetitive antagonists (Giraudat et al., 1986, 1987, 1989; Hucho et al., 1986; Pedersen & Cohen, 1992; White & Cohen, 1992) and functional expression of mutant AchRs (Charnet et al., 1990; Imoto et al., 1986, 1988, 1991; Villarroel & Sakmann, 1992) provide strong evidence that M2 segments from each subunit associate at the central axis to form at least part of the ion channel and also suggest that M2 regions are α-helical. In the absence of agonist, conserved aliphatic residues from each subunit (in δ, Leu-265 and Val-269) appear to associate to form the permeability barrier in the ion channel [White & Cohen, 1992; but also see Akabas et al. (1992)].

The M1, M3, and M4 segments must each have some contact with lipid, since they all contain sites of incorporation of a hydrophobic photoactivatable probe 1-azidopyrene (Blanton & Cohen, 1992). Because the M4 segment is the most hydrophobic yet has the lowest level of side chain conservation across species, this segment was proposed to have the largest contact with lipid [reviewed in Popot and Changeux (1984)]. Consistent with this proposal is the fact that α-M4 (but not M1, M2, or M3) can be replaced by a foreign hydrophobic segment without loss of AchR functionality (Tobimatsu et al., 1987).

Identification of lipid-exposed residues within α-M4, by use of the photoactivatable hydrophobic probe 3-trifluoromethyl-3-(*m*-[^{125}I]iodophenyl) diazirine ([^{125}I]TID), provided direct evidence that α-M4 is α-helical with a broad "face" exposed to lipid (Blanton & Cohen, 1992). Recently, however, it has been suggested that the M2 segments may be the only α-helical transmembrane segments. In the three-dimensional structure of the AchR at 9-Å resolution obtained by electron micrograph image reconstruction of tubular arrays of *Torpedo* postsynaptic membranes (Unwin, 1993), a single α-helix was identified in each subunit in the membrane-spanning region. The five helices, which were associated at the central axis lining the pore of the ion channel, were presumably M2 segments from each subunit. Each of the helices was flanked on the lipid-facing side by a continuous rim of density. Since α-helices were not observed in this region, the density was presumed to reflect β-sheets. Clearly, the proposition that the M1, M3, and M4 segments are comprised of β-sheets rather than α-helices has profound implications not only concerning the structure of the AchR and other ligand-gated ion channels but also for the vast majority of membrane

† This research was supported in part by USPHS Grant NS 19522 and by an award in Structural Neurobiology from the Keck Foundation. M.P.B. was supported in part by Training Grant NS 07009-13.

® Abstract published in *Advance ACS Abstracts,* February 15, 1994.

[1] Abbreviations: AchR, nicotinic acetylcholine receptor; 1-AP, 1-azidopyrene; [^{125}I]TID, 3-trifluoromethyl-3-(*m*-[^{125}I]iodophenyl)diazirine; SDS, sodium dodecyl sulfate; PAGE, polyacrylamide gel electrophoresis; OPA, ophthalaldehyde; V8 protease, *Staphylococcus aureus* V8 protease; PTH, phenylthiohydantoin; TPS, *Torpedo* physiological saline (250 mM NaCl, 3 mM $CaCl_2$, 2 mM $MgCl_2$, 5 mM sodium phosphate, pH 7.0).

0006-2960/94/0433-2859$04.50/0

proteins in which membrane-spanning α-helices are proposed on the basis of a stretch of hydrophobic amino acids of appropriate length.

We report here further analysis of the structure of the AchR protein-lipid interface by use of the photoactivatable, hydrophobic probe [^{125}I]TID. [^{125}I]TID-labeling of the AchR consists of both a specific (agonist- and TID-inhibitable) and a nonspecific component, indicative of its role as both a novel noncompetitive antagonist (White et al., 1991; White & Cohen, 1992) and as a hydrophobic probe [White & Cohen, 1988; White et al., 1991; see also McCarthy and Stroud (1989)]. The nonspecific component of [^{125}I]TID incorporation is consistent with photoincorporation into lipid-exposed regions of the AchR (White & Cohen, 1988; White et al., 1991; Blanton & Cohen, 1992). We characterize here the amino acids in the M1 segment of the α-subunit as well as in the M3 and M4 regions of each AchR subunit that are labeled nonspecifically by [^{125}I]TID. For α-M1, sites of reaction are restricted to four amino acids C-terminal to Pro-221. The distribution of labeled residues does not allow identification of secondary structure. For M3 segments the pattern of incorporation provides compelling evidence for α-helical secondary structure: the reactive residues would lie on a common "face" spanning 2 (α), 3 (β, γ), and 4 (δ) adjacent helical turns. For α-M4, the same five amino acids are labeled nonspecifically as previously identified (Blanton & Cohen, 1992) in the presence of 6.5 μM [^{125}I]TID but in the absence of nonradioactive TID. These labeled residues would lie on the common "face" of an α-helix but on both "faces" of a β-sheet. For non-α-subunits, reactivity was limited to two or three residues per subunit, which included resdues in each subunit analogous to those labeled in α as well as residues in γ- and δ- at a position not reactive in the α-subunit.

EXPERIMENTAL PROCEDURES

Materials. [^{125}I]TID (10 Ci/mmol) was purchased from Amersham. Nonradioactive TID (~70 mM) was synthesized as described by White et al. (1991) and stored in 100% ethanol at −20 °C. 1-Azidopyrene was purchased from Molecular Probes. *Staphylococcus aureus* V8 protease was purchased from ICN Biochemicals and TPCK-treated trypsin from Worthington Biochemical Corporation. Genapol C-100 (10%) was purchased from Calbiochem. Prestained low molecular weight gel standards were purchased from Gibco-BRL.

AchR-Enriched Membranes. AchR-enriched membranes were isolated from the electric organ of *Torpedo californica* (Marinus Inc., Westchester, CA) according to the procedure of Sobel et al. (1977) with the modifications described previously (Pedersen et al., 1986). The final membrane suspensions in 36% sucrose/0.02% NaN_3 were stored at −80 °C under argon and contained 1–1.5 nmol of acetylcholine binding sites/mg of protein as measured by a direct [^{3}H]-acetylcholine binding assay (Dreyer et al., 1986).

Preparative Photolabeling of AchR-Enriched Membranes with [^{125}I]TID/1-AP. *Torpedo* membranes were incubated with [^{125}I]TID under several conditions. For any given condition 12–15 mg of AchR-enriched membranes (2 mg/mL) in *Torpedo* physiological saline (TPS, 250 mM NaCl, 5 mM KCl, 3 mM $CaCl_2$, 2 mM $MgCl_2$, 5 mM sodium phosphate, pH 7.0, and 0.02% NaN_3) was incubated with [^{125}I]TID at a final concentration either 2.6 or 6.5 μM in the presence or absence of 100 μM carbamoylcholine and of a ~20-fold excess of nonradioactive TID. After a 30-min incubation, suspensions were irradiated for 15 min at a distance of less than 1 cm with a 365-nm lamp (EN-Spectroline). Following irradiation, each sample was pelleted (150000g) and then resuspended in TPS at a protein concentration of 2 mg/mL. 1-Azidopyrene was then added to the [^{125}I]TID-labeled membranes to a final concentration of 350 μM. After a 30-min incubation, membranes were once again irradiated for 15 min with a 365-nm lamp, and each sample was pelleted. Samples were then solubilized in sample loading buffer (Laemmli, 1970) and submitted to preparative SDS–PAGE.

Preparative SDS–Polyacrylamide Gel Electrophoresis. SDS–PAGE was performed as described by Laemmli (1970) using 3.0-mm thick 8% polyacrylamide gels with 0.33% bis-(acrylamide). Polypeptides incorporating 1-AP were visualized from their associated fluorescence when the gels were illuminated at 365 nm on a UV box, and the bands corresponding to AchR subunits were excised either for subunit isolation or for proteolytic digestion once the gel pieces were transferred to the wells of individual 15% mapping gels (Cleveland et al., 1977; Pedersen et al., 1986). Mapping gels were composed of a 4.5% acrylamide stacking gel and a 15% acrylamide separating gel. The gel pieces were overlaid with 350 μL of buffer (5% sucrose, 125 mM Tris-HCl, 0.1% SDS, pH 6.8) containing 250 μg of *S. aureus* V8 protease (500 μg of V8 protease for gel pieces containing the α-subunit). Electrophoresis was carried out overnight at 25 mA constant current. Previously, it was shown that when membranes were labeled separately with either 1-AP or [^{125}I]TID, the labeled material comigrated either as individual subunits or their V8 protease fragments (Blanton & Cohen, 1992; as well as present work). 1-AP/[^{125}I]TID-labeled fragments were visualized by the 1-AP associated fluorescence when gels were illuminated at 365 nm on a UV box, and the labeled bands were excised.

1-AP/[^{125}I]TID labeled subunits or proteolytic fragments were isolated from the excised gel pieces using a passive elution protocol similar to that described by Hager and Burgess (1988). The excised gel pieces were cut into small pieces and protein was eluted for 3–4 days into 20 mL of elution buffer (100 mM NH_4CO_3, 0.05% SDS, pH 7.8). The eluate was filtered (Whatman No. 1) and the protein concentrated using either a Centriprep-30 or -10 (Amicon). Excess SDS was removed by acetone precipitation (overnight at −20 °C). The amounts of recovered subunits or V8 protease fragments were determined by protein assay (Lowry et al., 1951).

Purification of Proteolytic Digests of [^{125}I]TID/1-AP Labeled Subunits and V8-Protease Fragments of Individual Subunits. For trypsin digestion, acetone-precipitated AchR subunits or V8 protease fragments of each subunit were resuspended in a small volume (~50 μL) of buffer (100 mM NH_4CO_3, 0.1% SDS, pH 7.8). The SDS concentration was then reduced by diluting with buffer without SDS, and Genapol C-100 (Calbiochem) was added, resulting in final concentrations of 0.02% SDS, 0.5% Genapol C-100, and 1–2 mg/mL of protein. Trypsin was added up to a total of 1:1 (w/w) enzyme to substrate ratio and incubated at room temperature for 3–4 days. For *S. aureus* V8 protease digestion, subunits or subunit proteolytic fragments were resuspended in 0.125 M Tris-HCl, 0.1% SDS, pH 6.8, at 1–2 mg/mL protein. V8 protease was added to a total of 1:1 (w/w) and incubated at room temperature for 3–4 days.

Both trypsin and V8 protease digests were separated on a Tricine gel system described by Schagger and von Jagow (1987). Gels were composed of a 10-cm long (1.5-mm thick) small pore separating gel (16.5% T/6% C), a 2-cm spacer gel (10% T/3% C), and a 2-cm stacking gel (4% T/3% C). Typically, a small aliquot of each digest (~5%) was first resolved on an analytical scale Tricine gel (1.0-mm thick),

and the autoradiograph of that dried gel was then used as a template to identify [^{125}I]TID-labeled bands when the rest of the digest was resolved on 1.5-mm preparative gels. This was done in conjunction with direct visualization of labeled fragments from the 1-AP associated fluorescence when gels were placed on a 365-nm UV box. [^{125}I]TID/1-AP labeled bands were then excised and the labeled polypeptides isolated from the gel pieces by passive elution. The molecular weights of labeled bands were estimated using prestained standards (Gibco-BRL): ovalbumin (43 000), carbonic anhydrase (29 000), α-lactoglobulin (18 400), lyzozyme (14 300), bovine trypsin inhibitor (6200), the A chain of insulin (3400), and the B chain of insulin (2300).

[^{125}I]TID/1-AP labeled fragments were further purified by reverse-phase HPLC using a Brownlee Aquapore C_4 column (100 × 2.1 mm). Solvent A was 0.08% TFA in water, and solvent B was 0.05% TFA in 60% acetonitrile/40% 2-propanol. The flow rate was maintained at 0.2 mL/min, and 0.5-mL fractions were collected. Prior to injection, material isolated from excised gel pieces was filtered (Whatman No. 1), the protein concentrated using a Centricon-3 (Amicon), and the material then spun briefly (15 000 rpm for ~10 s) in a table top microfuge to sediment any insoluble material. Peptides were eluted with a nonlinear gradient (Waters Model 680 gradient controller, curve No. 7) from 25% to 100% solvent B in 80 min. The elution of peptides was monitored by the absorbance at 210 nm and by fluorescence emission (357-nm excitation; 432-nm emission). The elution of [^{125}I]TID was monitored by γ-counting of the fractions.

Sequence Analysis. Amino-terminal sequence analysis was performed on either Applied Biosystems (ABI) Model 470A or 477A protein sequencers using gas phase cycles. Pooled HPLC samples were dried by vacumn centrifugation, resuspended in a small volume of 0.05% SDS (~20 μL) and immobilized on chemically modified glass fiber disks from Porton Instruments (Tarzana, CA), which were used rather than polybrene-treated filters in order to improve the sequencing yields of hydrophobic peptides (Pedersen et al., 1992). Approximately 30% of the released PTH-amino acids were separated by an on-line Model 120A PTH-amino acid analyzer, and approximately 60% was collected for determination of released ^{125}I by γ-counting with each sample counted for three 20-min intervals. Initial yield (I_o) and repetitive yield (R) were calculated by nonlinear least squares regression of the observed release (M) for each cycle (n): $M = I_oR^n$ (PTH derivatives of Ser, Thr, Cys, and His were omitted from the fit). In some cases, sequencing of some peptides was blocked by treatment of the Porton filter with *o*-phthalaldehyde (OPA). OPA reacts with primary, but not secondary, amines and can be used to block Edman degradation of any peptide not containing an N-terminal proline (Brauer et al., 1984). OPA treatment was carried out as described by Middleton et al. (1991) with the modifications described in White and Cohen (1992).

RESULTS

To identify the lipid-exposed residues in the AchR, AchR-rich membranes were incubated with [^{125}I]TID under three conditions: (1) in the presence of a 20-fold excess of nonradioactive TID, (2) in the presence of 100 μM carbamoylcholine, and (3) in the presence of 100 μM carbamoylcholine and a 20-fold excess of nonradioactive TID. For convenience, the following notation will be adopted to refer to these three labeling conditions: paired + and – signs separated by a slash will be used to indicate their presence or absence, respectively, of carbamoylcholine or TID, with the first sign indicating the presence or absence of carbamoylcholine, and the second the presence or absence of TID.

Sites of [^{125}I]TID Incorporation in M4 Regions of Each AchR Subunit. The M4 region of each subunit was isolated from membranes labeled in the absence or presence of 100 μM carbamoylcholine and in the presence of a 20-fold excess of nonradioactive TID ([–/+], [+/+]). M4 was isolated from a tryptic digest of the 10-kDa V8-protease fragment of α-subunit (α-V8–10; Asn-339 to Gly-437) as described previously (Blanton & Cohen, 1992). Tryptic digestion of α-V8–10 produced a fluorescent and radioactive band of 3–4 kDa (T-4) on a 16.5% T/6% C Tricine gel. When the material eluted from the T-4 band was further purified by reverse-phase HPLC (Figure 1A), both 1-AP fluorescence and ^{125}I counts eluted in a broad peak centered at 15 mL (~74% solvent B). When HPLC fractions 27–34 were pooled and subjected to N-terminal sequence analysis, a single sequence was evident beginning at Tyr-401 for T-4 labeled under either condition with initial yields of 137 ([–/+]) and 241 pmol ([+/+]) and repetitive yields of 87.5% ([–/+]) and 88.4% ([+/+]). The Tyr-401 sequence terminated at Arg-429 (1–2 pmol) and was present in a 10–20-fold greater abundance than any minor sequence. The pattern of ^{125}I release was complex but similar for both samples ([–/+] case shown in Figure 2A) and similiar to that seen for α-subunits isolated from receptor labeled in the absence of nonradioactive TID ([–/–], [+/–]; Blanton & Cohen, 1992). The largest release occurred in cycle 12, with additional release in cycles 15, 18, 22, and 25. Comparison of the pattern of release with the corresponding identified amino acids indicates that the labeled amino acids include Cys-412, Met-415, Cys-418, Thr-422, and Val-425.

The M4 regions of the β-, γ-, and δ-subunits were isolated from tryptic digests of the intact subunits isolated from membranes labeled under the same conditions ([–/+] and [+/+]) as the α-subunit. Small aliquots (5%) of each subunit digest were first resolved by analytical SDS–PAGE, and, on the basis of the autoradiograph of the dried gel, gel regions were selected to be excised when the bulk of each subunit digest was resolved on a 1.5-mm thick Tricine gel. Labeled material isolated from the gel slices from each region was further purified by reverse-phase HPLC and characterized by N-terminal sequence analysis.

For the β-subunit digest three gel regions were excised: region I (6–10 kDa, [–/+] 121 000 and [+/+] 123 000 cpm recovered); II (3.4–6 kDa, [–/+] 115 000 and [+/+] 110 000 cpm recovered); III (2–3.4 kDa, [–/+] 90 000 and [+/+] 92 000 cpm recovered). The β-subunit M4 region was identified in the material isolated from gel region II in HPLC fractions 25–29 (~60% solvent B, Figure 1B) which contained a fluorescence peak associated with a minor peak of ^{125}I counts.[2] For material isolated from both labeling conditions, fractions 25–29 contained as a primary sequence a peptide beginning at β-subunit Asp-427 (initial yields of 42 [–/+] and 55 pmol [+/+]; repetitive yields of 91% [–/+] and 92.5% [+/+]). A secondary sequence beginning at Lys-216 was present at half the mass level. Essentially the entire lengths of the M4 and

[2] In the material isolated from region II of the tryptic digest of the β-subunit, sequence analysis of the pool of HPLC fractions (22–24) containing the major peak of ^{125}I cpm revealed the presence of several peptides all of which could be attributed to fragments of trypsin. For the [+/+] sample there was a net release of ^{125}I in cycles 7 (16 cpm) and 12 (68 cpm) (16 600 cpm loaded, 8330 cpm retained following 20 cycles). No information is available for the [–/+] sample.

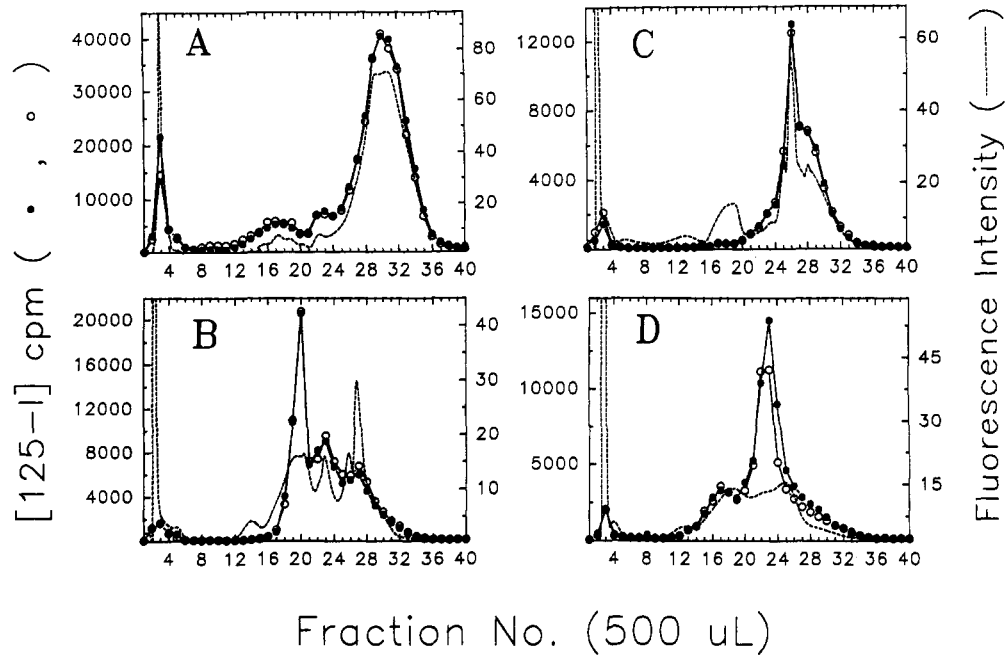

FIGURE 1: Reverse-phase HPLC purification of [^{125}I]TID/1-AP-labeled fragments from trypsin digests of α-V8–10 and of the β-, γ-, and δ-subunits. Membranes were labeled with [^{125}I]TID (6 μM) in the presence of 115 μM nonradioactive TID and in the absence (●, [−/+]) or presence (○, [+/+]) of carbamoylcholine. Tryptic digests of α-V8–10 (470 μg) and of the β-, γ-, and δ-subunits (~1000 μg each) were resolved on 1.5-mm thick 16.5% T/6% C Tricine gels. Gel fragment T-4 was isolated from the α-V8–10 digest; gel region II (3.4–6 kDa) was isolated from the β-subunit digest; gel region I (5–6 kDa) from γ; and gel region III (2–3.4 kDa) from δ. The labeled material was then further purified by reverse-phase HPLC on a Brownlee Aquapore C_4 column (100 × 2.1 mm) as described under Experimental Procedures. The elution of [^{125}I]TID/1-AP-labeled peptides was determined by monitoring the fluorescence emission intensity (dashed line; excitation, 357 nm; emission, 432 nm) and by γ-counting of the collected fractions (○, ●). (The fluorescence emission profile for the [−/+] condition is not shown.) Based upon the recovery of radioactivity, >90% of the material was recovered from the HPLC column.

M1 segments were contained within the 30 cycles of Edman degradation of the two peptides. The pattern of ^{125}I release was similar for both samples ([+/+] case shown in Figure 2B), with the largest release of ^{125}I occurring in cycle 15, along with clear release in cycles 21 and possibly 22. A peptide beginning at Lys-216 was also isolated by HPLC from gel region I (6–10 kDa) at mass levels similiar to that of the peptide in the sample of Figure 2B, but in this case no release of ^{125}I was detected during 26 sequencing cycles.[3] Therefore the release of ^{125}I seen at cycles 15 and 21–22 of Figure 2B would correspond to Tyr-441, Cys-447, and Ser-448 within the β-M4 region.

For the γ-subunit digests, the three gel regions excised were region I (5–6 kDa, [−/+] 76 000 and [+/+] 88 000 cpm recovered); II (3.4–5 kDa, [−/+] 117 000 and [+/+] 80 000 cpm); III (2–3.4 kDa, [−/+] 148 000 and [+/+] 108 000 cpm). The γ-M4 region was identified in material isolated from gel region I which contained a prominent fluorescent band. The HPLC chromatograph of the material repurified from this gel region (Figure 1C) contained a major fluorescent peak with an associated ^{125}I peak at 13 mL (~57% solvent B). Sequence analysis of the material in fractions 24–27 indicated the presence of a major sequence beginning at γ-subunit Val-446: (initial yields of 90 [−/+] and 72 pmol [+/+]; repetitive yields of 89.5% [−/+] and 90.6% [+/+]). This sequence was present in at least a 10-fold greater abundance than any secondary sequences. The pattern of ^{125}I release was similar for both samples ([+/+] case is shown in Figure 2C) with the largest release occurring in cycle 6, along with a small but significant release in cycle 15. Comparison of the pattern of release with the corresponding identified amino acids indicated that Cys-451 and Ser-460 within γ-M4 are labeled.

For the δ-subunit digests, the three gel regions excised were region I (5–9 kDa, [−/+] 155 000 and [+/+] 169 000 cpm recovered); II (3.4–5 kDa, [−/+] 170 000 and [+/+] 121 000 cpm); III (2–3.4 kDa, [−/+] 179 000 and [+/+] 203 000 cpm). The δ-M4 region was identified in HPLC fractions 21–24 (~50% solvent B) of region III which contained the major peak of ^{125}I counts but little fluorescence (Figure 1D). Sequence analysis of these pooled fractions established the presence of two sequences, the primary sequence began at Met-257 before M2: (initial yields of 116 [−/+] and 135 pmol [+/+]; repetitive yields of 88.5% [−/+] and 87.6% [+/+]); the secondary sequence began at Leu-456 (at the beginning of M4) with initial yields of 50 [−/+] and 67 pmol [+/+] and repetitive yields of 85.2% [−/+] and 85.4% [+/+]. For the [+/+] condition, major release of ^{125}I was detected in cycle 2 with additional release in cycles 6 and 10 (Figure 2D). For the [−/+] sample, there was similiar release in these cycles as well as release in cycles 9 and 13 at levels similiar to that seen in cycle 10 (data not shown). On the basis of previous analysis of the [^{125}I]TID incorporation into δ-M2 (White & Cohen, 1992; Figure 5), release in cycles 9 and 13 in the [−/+] condition originated from incorporation into Leu-265 and Val-269 of δ-M2, while the release in cycles 2, 6, and 10 seen for both samples indicated that Ser-457, Ile-461,[4] and Met-465 in the δ-M4 region are labeled nonspecicifically by [^{125}I]TID.

Isolation of Large V8 Protease Fragments of Each AchR Subunit. Limited digestion of AchR α-subunit with *S. aureus*

[3] [^{125}I]TID-labeled material [+/+] in gel region I was further purified by reverse-phase HPLC, and fractions 27–30 were pooled and sequenced with treatment with *o*-phthalaldehyde (OPA; see Experimental Procedures) at cycle 2. Following OPA block the only sequence present was that of Lys-216 (initial yield, 28 pmol; repetitive yield, 88.7%). No release of ^{125}I counts above background was detected in any cycle (14 483 cpm loaded and 8269 cpm retained on the filter after 26 cycles).

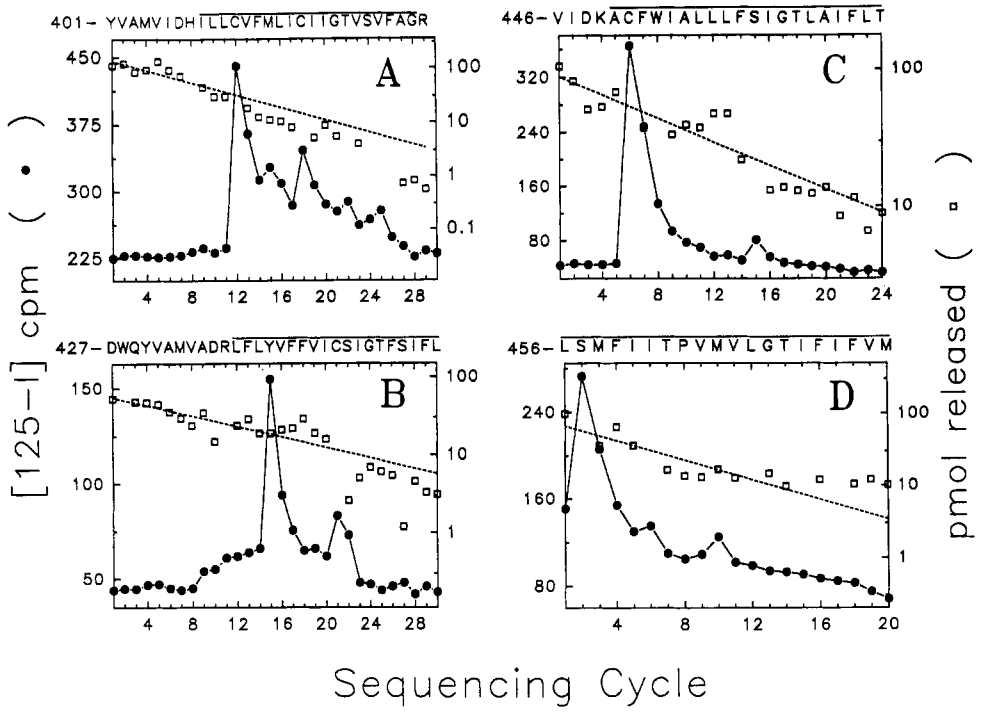

FIGURE 2: Radioactivity and mass release upon sequential Edman degradation of [^{125}I]TID/1-AP-labeled fragments containing M4 isolated from tryptic digests of α-V8–10 and of the β-, γ-, and δ-subunits. (Panel A) α-Subunit tryptic peptide T-4 isolated by HPLC (Figure 1A, fractions 27–34) from membranes labeled with [^{125}I]TID in the [–/+] condition (126 000 cpm loaded on the filter; 44 000 cpm remaining after 30 cycles). The only sequence detected began at Tyr-401 (initial yield, 140 pmol; repetitive yield, 87.5%). (Panel B) β-Subunit [+/+] material isolated by HPLC (Figure 1B, fractions 25–29) from gel region II (3.4–6 kDa) (16 550 cpm loaded on the filter; 6280 cpm remaining after 30 cycles). The primary sequence began at Asn-427 before M4 (initial yield, 55 pmol; repetitive yield, 92.5%). A secondary sequence was also present beginning at Lys-216 before M1 (initial yield, 26 pmol; repetitive yield, 86%). (Panel C) γ-Subunit [+/+] material isolated by HPLC (Figure 1C, fractions 24–27) from gel region I (5–6 kDa) (22 000 cpm loaded on the filter; 4790 cpm remaining after 24 cycles). The only sequence detected began at Val-446 (initial yield, 72 pmol; repetitive yield, 90.6%). (Panel D) δ-Subunit [+/+] material isolated by HPLC (Figure 1D, fractions 21–24) from gel region III (26 310 cpm loaded on the filter; 3185 cpm remaining after 20 cycles). The sequence beginning at Leu-456 (initial yield, 67 pmol; repetitive yield, 85.4%) was the secondary sequence detected; the primary sequence began at Met-257 before M2 (initial yield, 135 pmol; repetitive yield, 87.6%). For each sample 60% of each cycle of Edman degradation was analyzed for released ^{125}I (●) and 30% for PTH-amino acids (□) with the dashed lines corresponding to the exponential decay fit of the amount of detected PTH-amino acids for the peptides containing M4. The amino acid sequence of the sequenced peptide containing the M4 region is shown above each panel, with the solid line indicating the limits of the M4 regions.

V8 protease ("Cleveland Map") has been shown to produce reproducibly four principal fragments that run on a 15% SDS–polyacrylamide gel with apparent molecular weights of 20 000 (V8–20), 18 000 (V8–18), 10 000 (V8–10), and 4000 (V8–4) (Pedersen et al., 1986; White & Cohen, 1988). The V8–20 fragment contains the hydrophobic segments M1, M2, and M3 in a peptide which begins at Ser-162/Ser-173 and which terminates at or near the amino terminus of the V8–10 fragment (Glu-338/Asn-339). The V8–10 fragment contains the hydrophobic segment M4 and extends to the carboxy terminus of the α-subunit. The V8–18 fragment contains the N-linked carbohydrate of the α-subunit in a peptide beginning at Val-46/Thr-52 and terminates at or near the amino terminus of V8–20. Finally V8–4 contains the amino terminus of the α-subunit beginning at Ser-1.

This method was extended to the β-, γ-, and δ-subunits of AchR labeled by [^{125}I]TID and 1-AP. Two or three principal fluorescent bands were visible for each of the AchR subunits when the 15% polyacrylamide gels were placed on a 365-nm UV box. On the basis of the migration of each fragment relative to the fluorescent bands of α-V8–20 and α-V8–10, the bands were designated β-V8–22, β-V8–12, γ-V8–24, γ-V8–14, γ-V8–12, δ-V8–20, δ-V8–12, and δ-V8–11. Material in each of the bands was isolated, purified by HPLC, and subjected to N-terminal sequence analysis. For each fragment amino termini were determined to begin at β-V8–22 (Ile-173/Asn-183), β-V8–12 (Met-384/Ser-417), γ-V8–24 (Ala-167/Trp-170), γ-V8–14 (Leu-373/Ile-413), γ-V8–12 (Ala-1 of the β-subunit of the *Torpedo* Na/K ATPase), δ-V8–20 (Ile-192), δ-V8–12 (Ile-192), and δ-V8–11 (Lys-436). As a clear indication of the high degree of homology between the subunits, the amino termini of β-V8–22, γ-V8–24, and δ-V8–20 are within a few residues of the amino termini of α-V8–20 (in the aligned sequences), and each contained the M1, M2, and M3 regions. Similarly, β-V8–12, γ-V8–14, and δ-V8–11 contained the M4 regions and were analogs of α-V8–10.

Sites of [^{125}I]TID Incorporation in M4 Regions: V8 Protease Digestion of α-V8–10 and γ-V8–14. The M4 region of the α-subunit was also isolated from a V8 protease digest of α-V8–10 [+/+]. A 3–4 day digestion of α-V8–10 produced a fluorescent band in the 2–5 kDa molecular mass range (V8–2–5) when the digest was resolved on a 16.5% T/6% C Tricine gel (Blanton & Cohen, 1992). When the labeled material isolated from the V8–2–5 band was further purified by reverse-phase HPLC, a major peak of fluorescence and ^{125}I counts eluted at 15 mL (~74% solvent B). N-terminal sequence analysis of the pool of HPLC fractions 28–32 revealed a single sequence beginning at Trp-399 ([+/+] initial yield, 180 pmol;

[4] In the material isolated from region III of the tryptic digest of the δ-subunit (HPLC fractions 21–24), the possibility exists that the release of ^{125}I counts in cycle 6 reflects the presence of an undetected amount of the γ-M4 peptide from which release in cycle 6 would correspond to incorporation into γ-Cys-451 and not δ-Ile-461. On the basis of the results in Figure 2C, the presence of 3 pmol of γ-M4 would result in release of ~20 cpm in cycle 6.

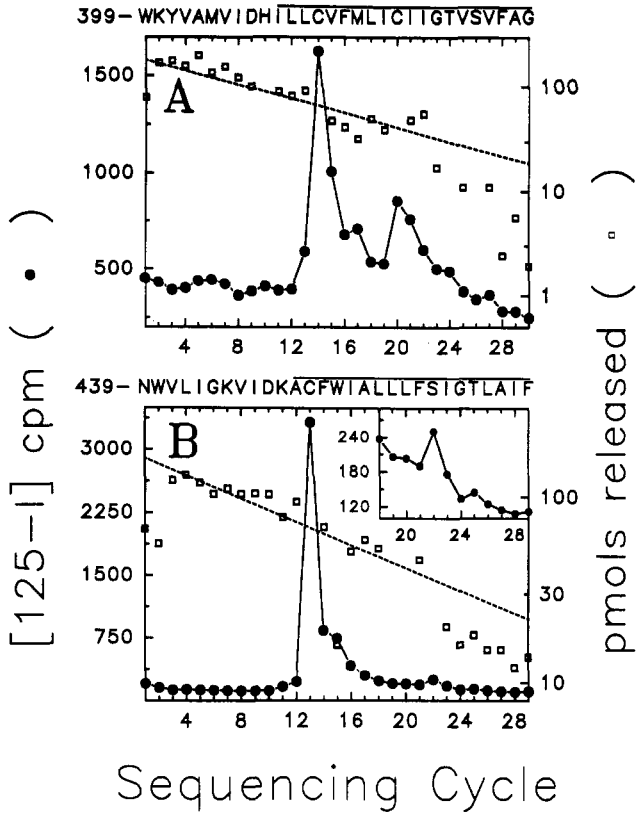

FIGURE 3: Radioactivity and mass release upon sequential Edman degradation of [^{125}I]TID/1-AP-labeled M4 fragments isolated from V8 protease digests of α-V8–10 and of γ-V8–14. V8 protease digests of α-V8–10 [+/+] and γ-V8–14 [+/+] were fractionated by Tricine gel SDS–PAGE and fragments α-V8–2–5 and γ-V8–6.3 containing ^{125}I and 1-AP were isolated and repurified by HPLC. (Panel A) α-V8–2–5 (HPLC fractions 28–32; 112 000 cpm loaded on the filter; 42 545 cpm remaining after 30 cycles). A single sequence was detected beginning at Trp-399 (initial yield, 180 pmol; repetitive yield, 92.2%). (Panel B) γ-V8–6.3, HPLC fractions 27–31 (38 880 cpm loaded on the filter; 12 342 cpm remaining after 30 cycles). A single peptide was detected beginning at γ-Asn-439 (initial yield, 160 pmol; repetitive yield, 93.0%). For each sample 60% of each cycle of Edman degradation was analyzed for released ^{125}I (●) and 30% for released PTH-amino acids (□) with the dashed lines corresponding to the exponential decay fit of the amount of detected PTH-amino acids. The amino acid sequence of each peptide containing the M4 region is shown above each panel with the solid line indicating the limits of the M4 regions.

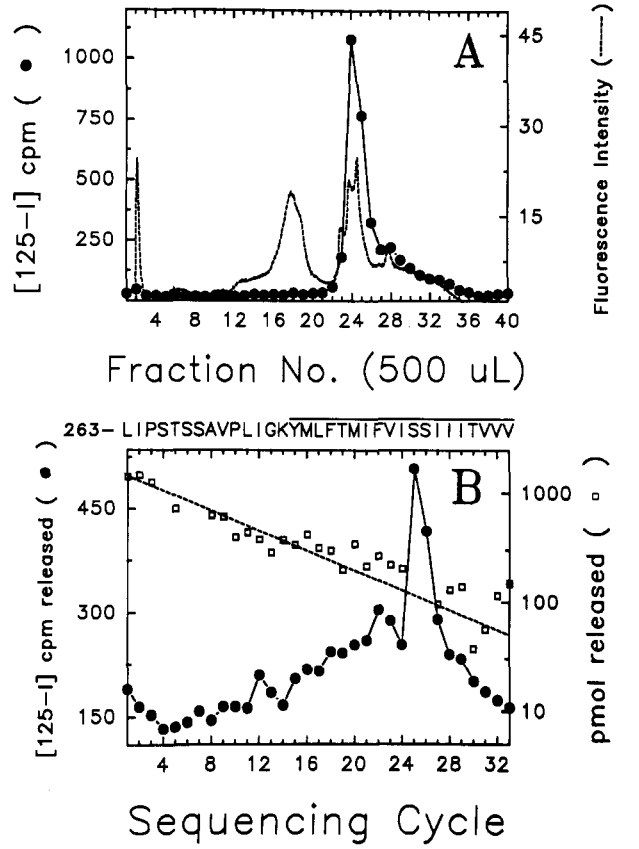

FIGURE 4: Reverse-phase HPLC purification and sequential Edman degradation of a [^{125}I]TID/1-AP-labeled fragment containing α-subunit M3. α-subunit fragment V8–9.4 isolated by Tricine gel SDS–PAGE from a V8 protease solution digest of α-V8–20 [+/–] was further purified by reverse-phase HPLC (panel A) as described under Experimental Procedures. Elution of ^{125}I was determined by counting 25 μL of each 500-μL fraction; recovery of ^{125}I cpm from the column was greater than 90%. HPLC fractions 22–26 were pooled and sequenced (panel B; [+/–]: 36 500 cpm loaded on the filter; 17 200 cpm remaining after 33 cycles). Thirty percent of each cycle of Edman degradation was analyzed for released PTH-amino acids (□) and 60% for ^{125}I (●). A single peptide was detected beginning at α-Leu-263 (initial yield, 1270 pmol; repetitive yield, 92.2%) which is shown above in panel B. The dashed line corresponds to the exponential decay fit of the amount of detected PTH-amino acids with the solid line indicating the limits of the M3 region.

repetitive yield, 92.2%). The largest ^{125}I release occurred in cycle 14 (Figure 3A), but there was also clear release in cycles 17 and 20 and detectable release in cycles 24 and 27. As for the M4 peptide isolated from a tryptic digest, comparison of the pattern of release with the corresponding identified amino acids indicates that the labeled amino acids include Cys-412, Met-415, Cys-418, Thr-422, and Val-425.

The M4 region of the γ-subunit was isolated from a V8 protease digest of γ-V8–14. A 3–4 day digestion of γ-V8–14 produced a fluorescent band of approximately 6.3 kDa (V8–6.3) when the digest was resolved on a 16.5% T/6% C Tricine gel (data not shown). When the labeled material isolated from the V8–6.3 band was further purified by reverse-phase HPLC, a major peak of fluorescence and ^{125}I counts eluted at 14.5 mL (~70% solvent B). N-terminal sequence analysis of the pool of HPLC fractions 27–31 indicated the presence of a single sequence beginning at Asn-439([+/+] initial yield, 160 pmol; repetitive yield, 93.0%). The largest ^{125}I release occurred in cycle 13 (Figure 3B), with additional low level release in cycles 15 and 25. Comparison of the pattern of release with the corresponding identified amino acids indicates that the labeled amino acids include Cys-451, Trp-453, and Ser-460.

Sites of [^{125}I]TID Incorporation in the α-M3 Region. The M3 region of the α-subunit was isolated from a V8 protease digest of α-V8–20 [+/–]. A 3–4 day digestion of α-V8–20 produced two fluorescent bands on a 16.5% T/6% C Tricine gel with apparent molecular masses of 9.4 (V8–9.4) and 7.0 (V8–7) kDa (Blanton & Cohen, 1992). When the material from the α-V8–9.4 band was isolated and further purified by reverse-phase HPLC (Figure 4A), there was both a peak of fluorescence and of ^{125}I counts eluting at 12 mL (~55% solvent B). When HPLC fractions 22–26 were pooled and sequenced, a single sequence was evident beginning at Leu-263 ([+/–] initial yield, 1265 pmol; repetitive yield, 92.2%) that was present in at least a 50–100-fold greater abundance than any minor sequences. The pattern of ^{125}I release was complex (Figure 4B), with the largest release of ^{125}I occurring in cycle 25. The complex release profile seen between cycle 15 and 21 precluded simple interpretation, but there was clear, low level release in cycles 12 and 22. Comparison of the pattern of ^{125}I release with the corresponding identified amino acids indicates that the labeled amino acids include Ile-274, Phe-284, and Ser-287.

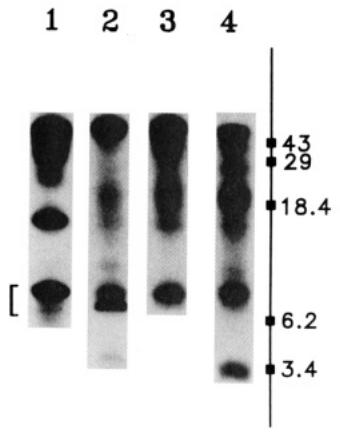

FIGURE 5: Proteolytic mapping the sites of [^{125}I]TID/1-AP incorporation into α-V8–20, β-V8–22, γ-V8–24, and δ-V8–20 using V8 protease. AchRs were labeled in the [+/+] condition, and α-V8–20, β-V8–22, γ-V8–24, and δ-V8–20 were isolated from a limited digest of individual receptor subunits. Each of these fragments was then digested in solution with V8 protease as described under Experimental Procedures. Shown is an autoradiograph of a Tricine SDS–PAGE gel with lanes 1–4 containing aliquots (~5%) of the digests of the fragments of α-, β-, γ-, δ-subunits, respectively. Approximately 10 000 cpm was loaded per lane; 24-h exposure. The bracket on the left spans the α-V8–9.4 band which contains the α-M3 region. The corresponding bands in the digests of the other subunits are designated β-V8–6.8 (lower band in the doublet), γ-V8–7.5, and δ-V8–7.5. The migration of prestained molecular weight standards is indicated on the right.

When the material from the V8–7 band [+/–] was isolated and further purified by reverse-phase HPLC, there was both a prominent peak of fluorescence and a peak of ^{125}I counts eluting at 12.5–13 mL (~60% solvent B) (data not shown). When HPLC fractions 24–28 were pooled and sequenced, two sequences were evident: one beginning at Trp-176 (initial yield, 84 pmol; repetitive yield, 89.1%) and a second beginning at Leu-263 (initial yield, 44 pmol; repetitive yield, 92.8%). For the Trp-176 sequence, the 26 cycles of Edman degradation fell short of the start of the M1 region by about 10 residues but did include Cys-192 and -193. No significant release above background (60 cpm) was observed in any of the 26 cycles.

Sites of [^{125}I]TID Incorporation in the M3 Region of Each of the AchR Subunits. The M3 regions of each subunit labeled in the [+/+] condition were isolated from V8 protease digests of α-V8–20, β-V8–22, γ-V8–24, and δ-V8–20. When small aliquots of each digest (~5%) were fractionated on a 16.5% T/6% C Tricine gel (1.0-mm thick) and analyzed by autoradiography, the α-V8–9.4 band was readily identified (Figure 5, lane 1, brackets) and bands of similiar mobility were seen in the digests of β-V8–22 (lane 2), γ-V8–24 (lane 3), and δ-V8–20 (lane 4). When the bulk of each digest was resolved on semipreparative gels which were then illuminated on a 365-nm UV box, the α-V8–9.4 band was strongly fluorescent, and in each of the other digests there was a fluorescent band of similiar mobility although of less intensity. For the digest of β-V8–22, the lower of the two bands in the autoradiograph (Figure 5, lane 2) was fluorescent. Each of the fluorescent bands were excised and designated α-V8–9.4, β-V-6.8, γ-V8–7.5, and δ-V8–7.5. When the material from each band was isolated and further purified by reverse-phase HPLC, material isolated from α-V8–9.4 eluted as before (Figure 4A) with peaks of fluorescence and of ^{125}I counts at 12.5 mL (~55% solvent B). Material isolated from β-V-6.8 (Figure 6A), γ-V8–7.5 (not shown), and δ-V8–7.5 (Figure 6B), all contained peaks of fluorescence and ^{125}I counts eluting at approximately 13 mL (~60% solvent B).

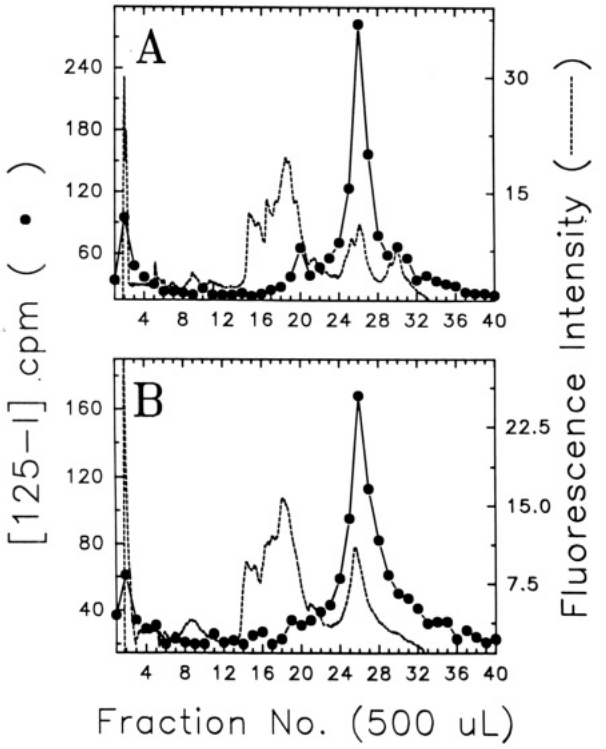

FIGURE 6: Reverse-phase HPLC purification of the [^{125}I]TID/1-AP-labeled fragments β-V8–6.8 and δ-V8–7.5 isolated from V8 protease digests of β-V8–22 and of δ-V8–20. The V8 protease fragments β-V8–6.8 and δ-V8–7.5 (Figure 5, lanes 2 and 4, respectively), isolated from exhaustive digests of β-V8–22 [+/+] and δ-V8–20 [+/+], were further purified by reverse-phase HPLC as described under Experimental Procedures and in the legend for Figure 1. The ^{125}I and 1-AP fluorescence elution profile for β-V8–6.8 and for δ-V8–7.5 are shown in panels A and B, respectively. Aliquots (25 μL) of each fraction were counted (●); for both digests recovery of ^{125}I cpm from the column was >90%.

N-terminal sequence analysis of the pool of HPLC fractions 22–26 from α-V8–9.4 indicated the presence of a single sequence beginning at Leu-263 ([+/+] initial yield, 275 pmol; repetitive yield, 89.4%) which was present in at least a 20-fold greater abundance than any other sequences. The pattern of ^{125}I release (Figure 7A) was essentially the same as that observed in the [+/–] condition (Figure 4B), with the largest release occurring in cycle 25 and clear release in cycles 12 and 22. There also appeared to be release in cycles 15 and 18. Comparison of the ^{125}I release with the corresponding identified amino acids indicates that the labeled amino acids include Ile-274, Tyr-277, Phe-280, Phe-284, and Ser-287.

Sequence analysis of the pool of HPLC fractions 24–28 from β-V8–6.8 established the presence of a single sequence beginning at Thr-273 ([+/+] initial yield, 165 pmol; repetitive yield, 92.7%), present in at least a 30-fold greater abundance than any minor sequences. The pattern of ^{125}I release (Figure 7B) was simpler than that of α-M3 with the largest release occurring in cycle 25 and with release in cycles 13 and 17. Release at those cycle indicates reaction of [^{125}I]TID with β-Met-285, β-Ile-289, and β-Phe-293.

Sequence analysis of the pool of HPLC fractions 24–28 from γ-V8–7.5 also established the presence of a single peptide that began at γ-Thr-276 ([+/+] initial yield, 53 pmol; repetitive yield, 92.0%) that was present at a 10–20-fold greater abundance than any other sequences. The largest release of ^{125}I (Figure 7C) was in cycle 25, with additional release in cycles 9, 17, and 21. ^{125}I release in those cycles indicates that labeled amino acids include γ-Ile-283, γ-Phe-292, γ-Leu-296, and γ-Asn-300. In addition, the release of ^{125}I in cycle

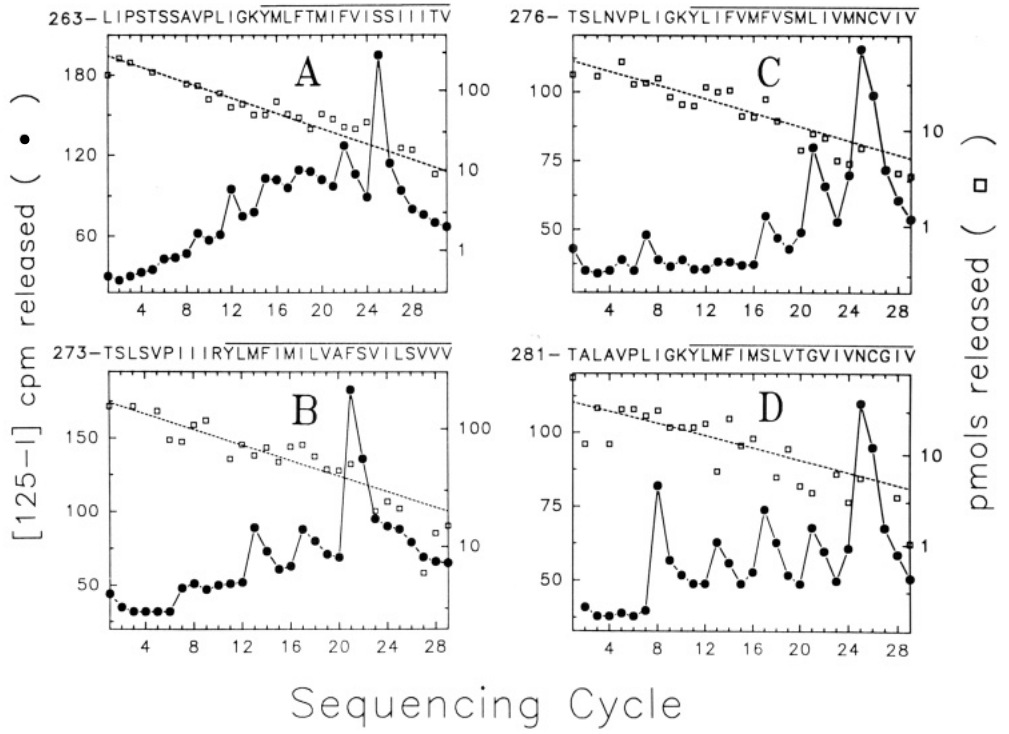

FIGURE 7: Radioactivity and mass release upon sequential Edman degradation of [^{125}I]TID/1-AP-labeled fragments containing M3 regions of each AchR subunit. The V8 protease fragments α-V8–9.4, β-V8–6.8, γ-V8–7.5, and δ-V8–7.5 (Figure 5) isolated from membranes labeled with [^{125}I]TID in the [+/+] condition were further purified by reverse-phase HPLC with fractions 22–26 pooled and sequenced for α-V8–9.4 (panel A) and fractions 24–28 pooled and sequenced for β-V8–6.8 (panel B), γ-V8–7.5 (panel C), and δ-V8–7.5 (panel D). The cpm loaded onto each filter and the cpm remaining after the number of cycles of Edman degradation given in parenthesis was as follows: α, 16 200 and 7300 (31); β, 11 040 and 5390 (29); γ, 8610 and 3400 (29); δ, 8340 and 3190 (29). For each sample 30% of each cycle of Edman degradation was analyzed for released PTH-amino acids (□) and 60% for ^{125}I (●). The dashed lines correspond to the exponential decay fits of the amount of detected PTH-amino acids and correspond to initial yields of 275 (A), 165 (B), 53 (C), and 38 pmol (D) and repetitive yields of 89.4%, 92.7%, 92.0%, and 92.4%, respectively. For each sample a single peptide was detected that began after a glutamate residue preceding M3; the amino acid sequence of each peptide is shown above each panel with the solid line indicating the limits of the M3 regions.

24, in the absence of any "preview" of Asn-300 (cycle 25) in that cycle, indicates that [^{125}I]TID also reacts with γ-Met-299.

N-terminal sequence analysis of the pool of HPLC fractions 24–28 from δ-V8–7.5 established the presence of a single sequence beginning at Thr-281 ([+/+] initial yield, 38 pmol; repetitive yield, 92.4%) that was present in at least a 10-fold greater abundance than any secondary sequences. The prinicpal release of ^{125}I (Figure 7D) occurred in cycle 25, and there was also release in cycles 9, 13, 17, and 21. Thus within δ-subunit [^{125}I]TID reacted with Ile-288, Met-293, Ser-297, Gly-301, and Asn-305. In addition, the lack of "preview" of Asn-305 (cycle 25) in the previous cycle indicates that the ^{125}I release in cycle 24 represents [^{125}I]TID incorporation into Val-304.

Sites of [^{125}I]TID Incorporation in the α-M1 Region. The α-subunit M1 region can be isolated from a tryptic digest of α-V8–20 (Blanton & Cohen, 1992). In the present work, α-V8–20 was isolated from membranes labeled under two conditions ([−/+] and [+/+]) and digested with trypsin. When small aliquots (5%) of the digests were resolved on an analytical scale Tricine gel (1.0 mm), the autoradiograph of the dried gel (Figure 8) revealed the presence of a number of [^{125}I]-TID-labeled fragments. On the basis of this autoradiograph, four regions were excised when the bulk of the digests was resolved on a 1.5-mm thick Tricine gel (region I, ~30–45 kDa; II, 6–10 kDa; III, 3.4–6 kDa; IV, 2–3.4 kDa). Material isolated from each region was further purified by reverse-phase HPLC (Figure 9). The M1 region was identified by sequence analysis in HPLC fractions 24–28 (13 mL, ~57% solvent B) of the material from gel region III (Figure 9C).

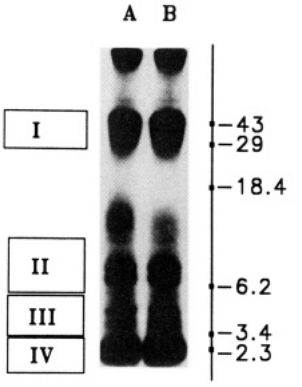

FIGURE 8: Proteolytic mapping the sites of [^{125}I]TID/1-AP incorporation in α-V8–20 using trypsin. Fragment α-V8–20, isolated from a limited V8 protease digest of α-subunit, was further digested with trypsin (100% w/w, 4 days) as described under Experimental Procedures. An aliquot (~5%) of each digest was resolved by SDS–PAGE on a 1.0-mm thick 16.5% T/6% C Tricine gel, and following electrophoresis the gel was subjected to autoradiography (48 h). Digests of α-V8–20 labeled under the [−/+] and [+/+] condition are shown in lanes A and B, respectively. When the bulk of the labeled material was resolved on a 1.5-mm thick 16.5% T/6% C Tricine gel, regions I–IV were excised from the gel: region I, ~30–45 kDa; II, 6–10 kDa; III, 3.4–6 kDa; IV, 2–3.4 kDa. For the preparative gel: ([−/+] condition) 42, 15, 16, and 15% of the loaded counts (540 000 cpm) were recovered in gel regions I, II, III, and IV, respectively; ([+/+] condition) 38, 16, 16, and 17% of the loaded counts (404 000 cpm) were recovered in gel regions I, II, III, and IV, respectively. The migration of prestained molecular weight standards is indicated on the right (see Experimental Procedures).

The fractions contained the major peak of ^{125}I counts and a sharp peak of fluorescence. In the sequence analysis of this

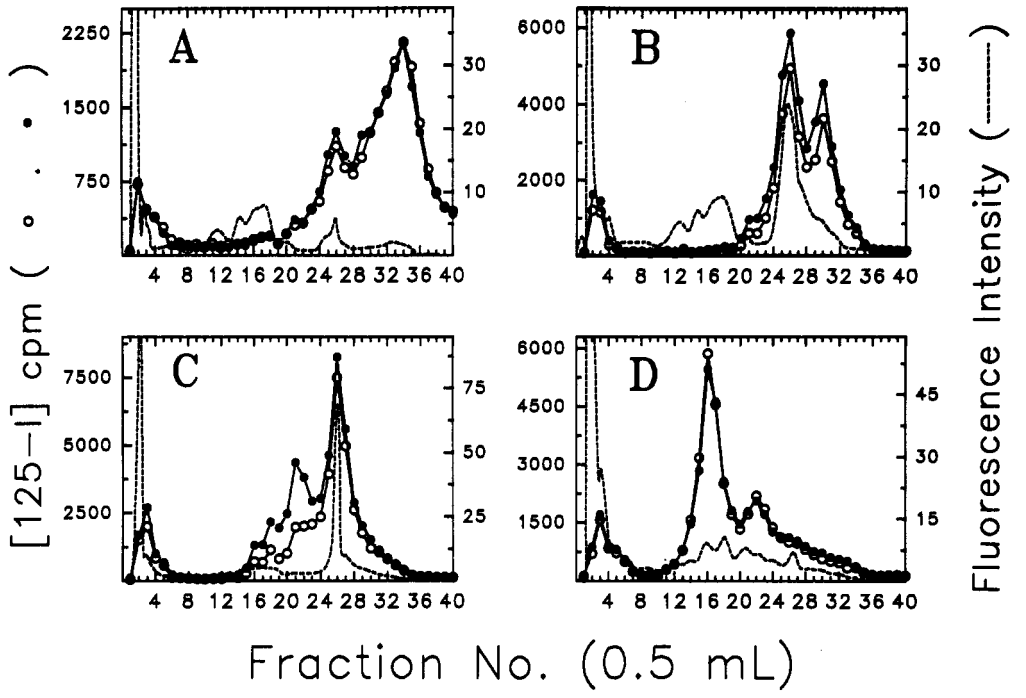

FIGURE 9: Reverse-phase HPLC purification of [^{125}I]TID/1-AP-labeled fragments from trypsin digests of α-V8–20. α-V8–20 was isolated from membranes labeled with [^{125}I]TID (6 μM) in the presence of 115 μM nonradioactive TID and in the absence (●, [−/+]) or prescence (○, [+/+]) of carbamoylcholine. Tryptic digests of α-V8–20 were resolved on 1.5-mm thick 16.5% T/6% C Tricine gels. The material eluted from gel regions I–IV (Figure 8) were each then purified by reverse-phase HPLC on a Brownlee Aquapore C_4 column (100 × 2.1 mm) as described under Experimental Procedures with elution profiles for regions I–IV shown in panels A–D, respectively (- - -, fluorescence; ○, ●, ^{125}I). Only the fluorescence profiles for the [−/+] condition are shown, and in the HPLC chromatographs shown in panel C the sensitivity of the fluorescence spectrophotometer was set at one-half the level as that used in the HPLC runs presented in panels A, B, and D. The recovery of ^{125}I cpm from the column was >90%, with the exception of the material isolated from gel region IV (panel A), which exhibited a rather poor column recovery (~40%).

material (Figure 10) the sequencing filters were treated with *o*-phthalaldehyde (OPA) in cycle 2 to block all sequences not containing an amino-terminal proline (see Experimental Procedures). The only sequence present after OPA treatment was that beginning at α-Ile-210 (initial yields of 198 [−/+] and 158 [+/+] pmol; repetitive yields of 91.9% [−/+] and 92.4% [+/+]). In fact, the PTH derivative of isoleucine observed in the first cycle of Edman degradation was actually present in at least a 20-fold greater abundance than any other PTH-amino acid derivatives arising from secondary sequences. The pattern of ^{125}I release was similar for material isolated from both labeling conditions (Figure 10). Approximately equal amounts of ^{125}I counts were released in cycles 13, 14, 18, and 19, consistent with reaction of [^{125}I]TID with Cys-222, Leu-223, Phe-227, and Leu-228 within the M1 region of the α-subunit.

The HPLC chromatograph of the aggregated material isolated from region I of the Tricine gel (Figure 8) contained a broad peak of ^{125}I counts eluting at 17 mL (~92% solvent B; Figure 9A) with an unusually poor recovery of ^{125}I counts (~40%). Sequence analysis of the pool of HPLC fractions 32–35 indicated the presence of peptides beginning at Ile-210 (before M1), Met-243 (before M2), and Tyr-277 before M3 in approximately equal abundance (I_0 = 10 pmol) for the [−/+] and [+/+] conditions.

The HPLC chromatograph of material from gel region II (6–10 kDa, Figure 9B) contained peaks of ^{125}I counts at 13 mL (~57% solvent B), eluting with a peak of fluorescence, and at 15 mL (~74% solvent B). Sequence analysis of the pool of HPLC fractions 24–28 indicated the presence of a primary sequence beginning at Ile-210 (initial yields of 45 [−/+] and 31 [+/+] pmol; repetitive yields of 95.9% [−/+] and 96% [+/+]. The pattern of ^{125}I release was similar for both conditions and was identical to that observed in Figure 10 for the M1 region isolated from gel region III (data not shown). Sequence analysis of the pool of HPLC fractions 29–32 indicated the presence of sequences beginning at Met-243 and Ile-210 at mass levels (~5 pmol) substantially lower than that of the Ile-210 sequence found in fractions 24–28, and the level of ^{125}I release in each cycle was less than 10 cpm. The presence in gel region II of two bands of ^{125}I with apparent molecular masses of 7.6 and 6.8 kDa (Figure 8) indicates that the sequence beginning at Ile-210 contains both the M1 and M2 regions (i.e., M1 + M2, Ile-210 to Lys-276; calculated M_r = 7274) while that beginning at Met-243 contains both the M2 and M3 regions (i.e., M2 + M3, Met-243 to Arg-301; calculated M_r = 6504).

The HPLC chromatograph of material isolated from gel region IV (2–3.4 kDa, Figure 9D) contained a peak of ^{125}I counts eluting at 8 mL (~37% solvent B) with no apparent peak of fluorescence. N-terminal sequencing of the pool of HPLC fractions 15–18 indicated the presence of a number of different sequences all of which could be attributed to fragments of trypsin. There was release of ^{125}I extending over cycles 2–11, with less than 10% of the counts initially loaded onto the sequencing filter retained after 24 cycles of Edman degradation. The relatively early elution of the ^{125}I counts from the reverse-phase HPLC column and the uncharacteristically low amount of ^{125}I counts remaining on the filter after 24 cycles suggest that this material may not represent [^{125}I]TID incorporation into a polypeptide region.

DISCUSSION

The studies presented here provide an extensive characterization of the structure of the *Torpedo* AchR at its lipid

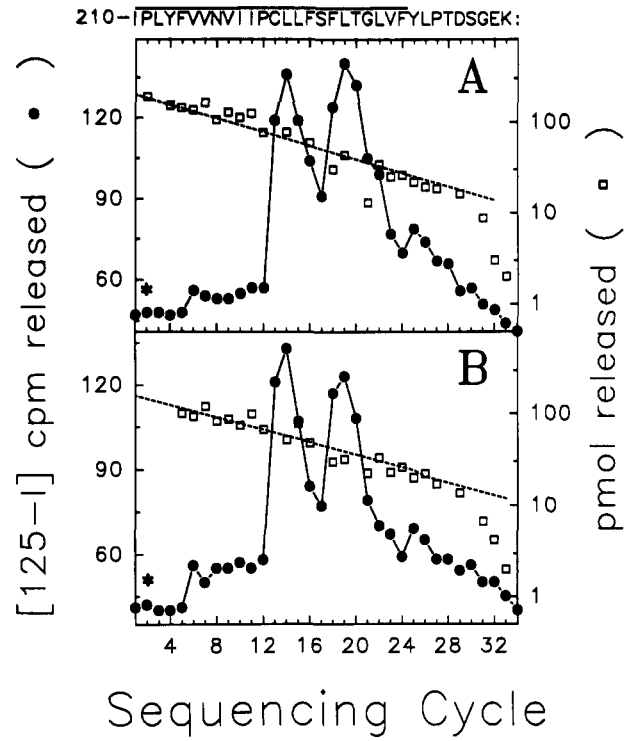

FIGURE 10: Radioactivity and mass release upon sequential Edman degradation of [^{125}I]TID/1-AP-labeled fragments containing M1 isolated from tryptic digests of α-V8–20. For the material isolated from gel region III, HPLC fractions 24–28 (Figure 9C) were pooled and subjected to N-terminal sequence analysis. (Panel A) [−/+] condition (20 700 cpm loaded on the filter; 6278 cpm remaining after 34 cycles). (Panel B) [+/+] condition (17 474 cpm loaded on the filter; 3756 cpm remaining after 34 cycles). After the first cycle of degradation, the sequencing filters were treated with *o*-pthalaldehyde (see Experimental Procedures) since cycle 2 corresponds to the exposure of a proline residue (*) in the observed primary sequence which began at Ile-210 before M1. The amino acid sequence of this peptide is shown above the panels with the solid line indicating the limits of the M1 region. Thirty percent of each cycle of Edman degradation was analyzed for released PTH-amino acids (□) and 60% for ^{125}I (●). The dashed lines correspond to the exponential decay fit of the amount of detected PTH-amino acids, with initial yields of 198 and 158 pmol for [−/+] and [+/+] conditions, respectively, and repetitive yields of 91.9 and 92.4%, respectively.

interface, including the first biochemical examination of the secondary structure of these membrane-spanning regions. The sites of [^{125}I]TID incorporation into the M4 region of the AchR α-subunit have now been determined under four different labeling conditions: in the presence [+/−] and absence [−/−] of carbamoylcholine (Blanton & Cohen, 1992) and now with the additional presence of an excess of nonradioactive TID ([−/+], [+/+]). In all four conditions the pattern of ^{125}I release was the same, indicating [^{125}I]TID incorporation into Cys-412, Met-415, Cys-418, Thr-422, and Val-425 within α-M4. Reaction of [^{125}I]TID with these residues was established by sequence analysis of peptides containing α-M4 isolated from tryptic (Figure 2A) and V8 (Figure 3A) digests of α-V8–10. [^{125}I]TID incorporation into each of these residues is inhibited neither by the presence of agonist nor by the presence of an excess of nonradioactive TID. Such nonspecific incorporation is expected for labeling at a lipid exposed region and would not be consistent with labeling of hydrophobic pockets within the protein interior where [^{125}I]TID binding would be inhibitable by excess nonradioactive TID. Based upon these criteria, the simplest interpretation is that the labeled residues are situated at the lipid–protein interface of the AchR.

The sites of [^{125}I]TID incorporation have now also been determined for the M4 regions of β-, γ-, and δ-subunits for the [−/+] and [+/+] conditions. The pattern of ^{125}I release in β-M4 indicates that [^{125}I]TID is incorporated nonspecifically into Tyr-441 and Cys-447, which are equivalent to the principal labeled residues in α-M4 (Cys-412 and Cys-418) and possibly into β-Ser-448. [^{125}I]TID reacted nonspecifically with Cys-451 and Ser-460 in γ-M4 (Figures 2C and 3B) and with Ser-457 and Met-465 in δ-M4. It is also possible that some of the ^{125}I release in cycles immediately following these labeled residues results from lower level reaction with the following amino acids. However, due to the lags resulting from the 90% repetitive yields inherent in the Edman degradation reaction, these cycles contain prior PTH-amino acids and associated ^{125}I, and this matter can not be resolved without direct characterization of the ^{125}I-labeled amino acids released in each cycle.

The sites of ^{125}I TID reactivity are summarized in Figure 11 where M4 segments are modeled as α-helices. It is striking that fewer labeled residues were detected in non-α-subunits than in α-subunit. This is unlikely to result simply from differences in intrinsic side chain reactivities that have been estimated by Sigrist et al. (1990) from the relative photoincorporation of a trifluoromethylphenyl diazirine into radiolabeled amino acids (Table 1). For example, unlabeled β-Phe-445, γ-Leu-456, and δ-Thr-462 that are positioned equivalently to labeled α-Met-415, all have carbene reactivities similar to that of Met. It is also striking that the positions most highly labeled in the β-subunit were the same as in the α-subunit and different from the sites of reaction in γ and δ. Despite the fact that Cys is 5–10 times as reactive as Tyr, Ser, or Met, ^{125}I incorporation in β-Tyr-441 relative to β-Cys-447 is quite similar to the incorporation seen in α-Cys-412 relative to α-Cys-418, and incorporation into δ-Ser-457 relative to δ-Met-465 is similar to that of γ -Cys-451 relative to γ-Ser-460. Thus positional effects rather than intrinsic side chain reactivities are likely to dominate the observed labeling patterns.

As noted before (Blanton & Cohen, 1992), the periodicity of [^{125}I]TID labeled amino acids within α-M4 argues that the region possesses α-helical secondary structure. The labeled amino acids would lie on a broad "face" of an α-helix distributed over five consecutive turns (Figure 11). In contrast, the distribution of labeled residues is inconsistent with the labeling of a single face of a β-sheet, since three labeled residues (Cys-412, Cys-418, and Thr-422) would lie on one face and Met-415 and Val-425 on the other. Interpretation of the α-subunit labeling pattern in terms of secondary structure models is complicated, however, by the fact that there are two α-subunits per AchR monomer that may be positioned and labeled nonequivalently. While the pattern of labeling of non-α-subunits could yield more constraints on secondary structure assignment, this was not so because only two or three residues were labeled in each subunit. However, the labeled residues can all be accommodated within a common, broadly exposed face of an α-helix.

In contrast to M4 segments, more side chains reacted with [^{125}I]TID in M3 segments of non-α-subunits than in α-M3. M3 segments were isolated from subunits by first generating 20-kDa fragments containing M1–M3 and then by digesting those fragments with V8 protease which produced fragments of ~8 kDa with N-termini between M2 and M3. For α-subunit, α-V8–9.4 was labeled in the presence of carbamoylcholine and in the absence or presence of excess nonradioactive TID ([+/−],[+/+], Figure 4) and also in the [−/+]

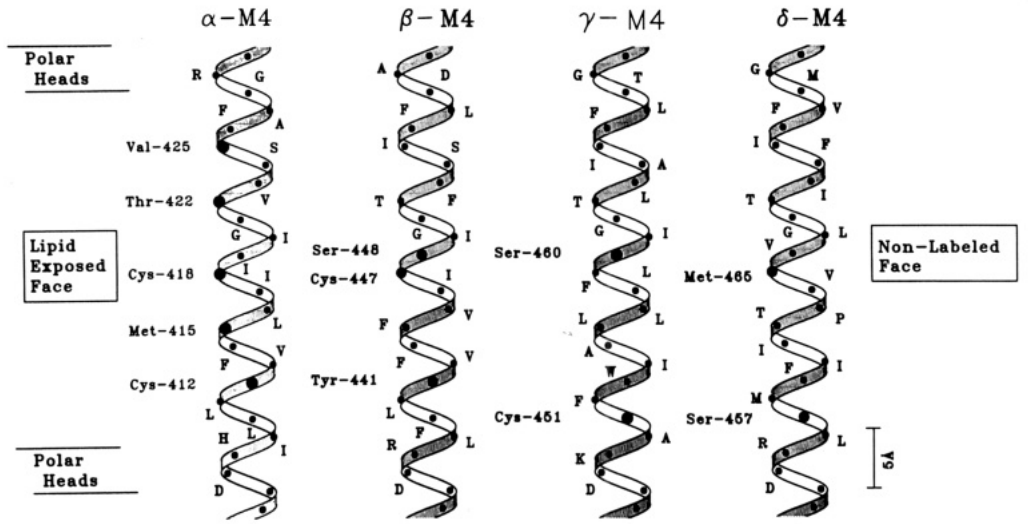

FIGURE 11: Helical representations of the α-, β-, γ-, and δ-subunit M4 regions. [^{125}I]TID-labeled amino acid residues are indicated along the left side of the helix along with the location of the labeled amino acid in the subunit primary sequence. Helices are oriented with N-termini at the bottom to reflect the extracellular location of the carboxy termini (DiPaola et al., 1989).

Table 1: Relative Reactivities of Amino Acid Side Chains with (Trifluoromethyl)phenylcarbene[a]

low	Gly(1), Gln(1), Glu(1), Arg(1), Ala(1), Val(2), Lys(2), Asn(2), Leu(2), Asp(2), Ile(2), Pro(2)
intermediate	Ser(3), Met(3), Thr(5), Phe(6), His(6), Tyr(6)
high	Trp(20), Cys(30)

[a] Based upon data of Sigrist et al. (1990). Side chain reactivity was based upon photoinduced reactivity of radiolabeled amino acids with 3-(trifluoromethyl)-3-(*m*-isothiocyanophenyl)diazirine covalently coupled to glass filters.

and [+/+] conditions (Figure 7A). The pattern of ^{125}I release was the same for all labeling conditions, consistent with labeling of residues within M3 at the protein–lipid interface. The principal sites of reaction were α-Phe-284 and α-Ser-287. There was also lower level reactivity with residues N-terminal to Phe-284, with Tyr-277 and Phe-280 probably labeled, but the complexity of the ^{125}I release pattern makes interpretation difficult. For β-, γ-, and δ-subunits, M3 segments were isolated from AchRs labeled in the presence of excess nonradioactive TID ([−/+], [+/+]). The patterns of ^{125}I release (Figure 7B–D) were simpler than that of α-M3 and indicate reaction with Met-285, Ile-289, and Phe-293 in β-M3, with Phe-292, Leu-296, Met-299, and Asn-300 in γ-M3, and into Met-293, Ser-297, Gly-301, Val-304, and Asn-305 in δ-M3.

The distribution of labeled reidues is summarized in Figure 12 where the M3 segments are modeled as α-helices. Within M3 segments the most highly labeled amino acids (γ-Leu-296, γ-Asn-300, δ-Gly-301, δ-Asn-305) are in fact side chains possessing the lowest intrinsic reactivities toward carbenes (Table 1), and they are positioned within the primary structure in the midst of unlabeled side chains of high reactivity such as γ-Met-291 and δ-Thr-300 and, in particular, γ-Cys-301 and δ-Cys-306 which, if labeled at all, are labeled at substantially lower level than the preceding Asn. There are clear gradients in the extent of labeling of M3 residues that are independent of side chain reactivity. Reaction with δ-Asn-305 (19 cpm/pmol) is 5-fold higher than with δ-Met-293 (4 cpm/pmol) and similar gradients exist for β- and γ-subunits. Such gradients suggest that TID concentration is higher near the middle of the bilayer than at the N-terminal (extracellular) end. For M4 segments, where side chains near the N-termini (cytoplasmic ends) were labeled, the gradient was less evident.

The periodicity of [^{125}I]TID-labeled amino acids within each M3 region argues strongly that the region possesses α-helical secondary structure. Arguments in favor of α-helix and inconsistent with β-sheet can be summarized. (1) For M3 of β-, γ-, and δ-subunits, each of the [^{125}I]TID-labeled residues will lie on a single homologous face of an α-helix extending over three (β,γ) or four (δ) consecutive turns. Adjacent labeled residues such as Met-299 and Asn-300 in γ-M3 define a labeled face while lack of reaction with γ-Cys-301 defines an inaccessible face. (2) If M3 segments are modeled as β-sheets, the labeled residues would neither be restricted to a single face nor would they define a continuous, labeled surface. In γ (or δ)-subunit the three (or four) principal labeled residues would lie on a common surface, but γ-Met-295 and γ-Met-299, as well as δ-Val-304, would lie on the other side. Along the labeled face of a γ- or δ-M3 β-sheet, labeled residues would alternate with unlabeled residues, i.e., γ-Ser-294, γ-Val-298, δ-Ile-295, δ-Val-299, and δ-Val-303 are all unlabeled. It is difficult to envision how different polypeptide regions could interact to generate alternating ridges of a β-sheet not exposed to lipid. (3) In α-M3 the labeled residues Phe-284 and Ser-287 would lie on opposite sides of a β-sheet.

Our conclusion that M3 and M4 segments are α-helical is in apparent contradiction with the results of Unwin (1993), who reported the presence of 5 α-helices in the AchR transmembrane region, each located at the central axis and presumed to be M2 segments from each subunit. Lack of similar density profiles at the AchR periphery led to the suggestion that the remaining segments might be β-sheet. We suggest that the α-helices at the periphery are undetected at the resolution currently available (9 Å) because secondary structure elements at the protein–lipid interface are less highly ordered than at the central axis of the AchR. Higher resolution structural analyses as well analysis of the pattern of labeling by other reactive hydrophobic probes will clarify this matter.

In addition to the labeling within M3 summarized in Figure 12, there was clear reactivity (Figure 7) of [^{125}I]TID with residues in each subunit immediately preceeding the Gly/Lys(Arg) defining the beginning of M3. Labeled residues include δ-Ile-288 (cycle 8), γ-Leu-282 (cycle 7), α-Ile-274 (cycle 12), and possibly β-Ile-279 and -280 (cycles 7 and 8). If included within the α-helix, they would all lie on the face opposite to all the other labeled residues in M3. Since these labeled residues are positioned between a Pro and a Gly, they

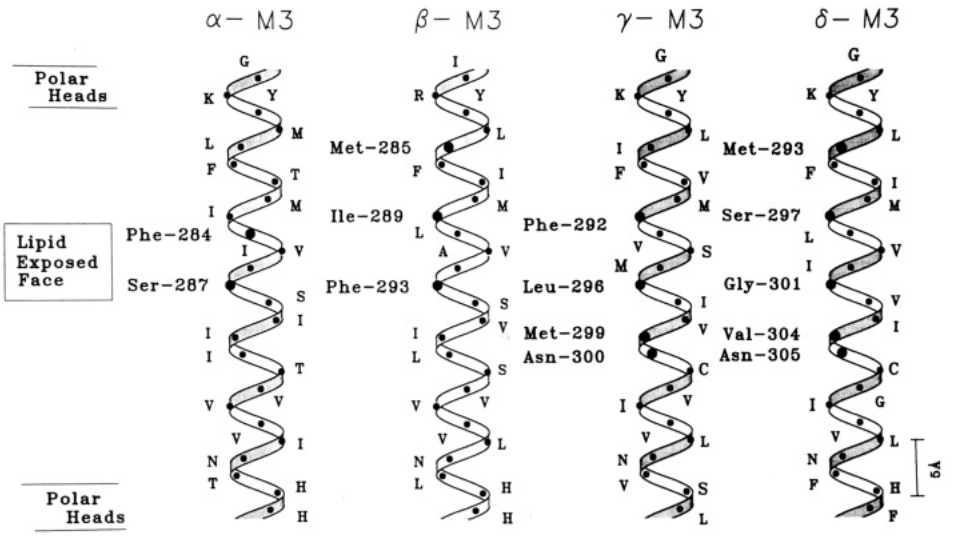

FIGURE 12: Helical representations of the α-, β-, γ-, and δ-subunit M3 regions. [^{125}I]TID-labeled amino acid residues are indicated along the left side of the helix along with the location of the labeled amino acid in the subunit primary sequence. Helices are oriented with N-termini at the top to reflect accessibility from the extracellular side to the charged residues at the C-termini of M2 segments (Imoto et al., 1988).

```
                 E LIPSTSSAVPLIGK
---M2---         DKV PETSLSVPTTIR      ---M3---
                 QKV PETSLNVPLIGK
                 QRL PETALAVPLIGK
```

FIGURE 13: [^{125}I]TID incorporation into residues of the M2/M3 loop region. N-terminal sequence analysis of peptides containing the M3 region (Figures 4B and 7) revealed [^{125}I]TID incorporation into α-Ile-274, β-Ile-279 and Ile-280, γ-Leu-282, and δ-Ile-288. The amino acid residues comprising the short loop region between the hydrophobic region M2 and M3 of the aligned subunit sequences are shown with the [^{125}I]TID-labeled amino acids indicated with an overstrike.

are likely to reflect labeling of a turn region in contact with lipid. For each subunit these labeled residues are conserved across species, and the 13 amino acids in the M2–M3 "loop" show the same extent of conservation across species as do the corresponding M3 segments.

Independent of secondary structure assignment, the pattern of nonspecific photolabeling of M3 and M4 segments leads to several conclusions about the structure of the AchR protein–lipid interface. While it has been predicted that the external faces of transmembrane α-helices should be the most hydrophobic (Engelman & Zaccai 1980; von Heijne, 1986) as is seen in the bacterial photosynthetic reaction center (Rees et al., 1989), this is not simply the case for AchR M3 or M4 segments. For M4, while both faces are comprised of hydrophobic residues, it is the face not labeled by [^{125}I]TID that is comprised almost exclusively of aliphatic residues, while for M3 segments there are polar residues on labeled and unlabeled faces. Interestingly, the nonlabeled face of δ-M4 contains a proline residue (Pro-463). The proline nitrogen lacks a proton so that the proline peptide bond cannot participate in hydrogen bonding to a neighboring carbonyl group within the α-helix. However, if this face of the helix is packed toward the protein interior, the unsatisfied hydrogen bond can be satisfied by making contacts with other protein segments. In an analysis of proline-containing transmembrane helices, von Heijne (1991) concluded that such helices tend to be oriented with the convex proline-containing side packed toward the protein interior. Comparison of the primary structures of the transmembrane α-helices in the photosynthetic reaction centers establishes that lipid-accessible residues are less conserved across species and have different substitution patterns than inaccessible residues in soluble proteins (Donnelly et al., 1993). The hydrophobic segments M1–M4 of AchR subunits are highly conserved across species. M4 segments are the least conserved with 62% and 45% identity for six muscle type α- and δ-subunits, while for α-M3 and δ-M3, 88% and 58% of positions are identical [reviewed in Cockcroft et al. (1992)]. The high degree of conservation precludes ready prediction of a lipid-exposed surface, although it is noteworthy that in δ-M3 four of the five labeled residues are at positions that are not conserved.

The distribution of [^{125}I]TID labeled residues in M4 segments is consistent with the notion that M4 segments are the transmembrane segments with greatest contact with lipid [reviewed in Popot and Changeux (1984)]. Substitution of α-Cys-418, which is labeled by [^{125}I]TID, by Trp results in a 20-fold increase in channel open time with little alteration of channel conductance (Li et al., 1992). Thus, despite the fact that this Cys is conserved in all muscle type α-subunits, the structure of a residue at the protein–lipid interface does affect channel gating. On the basis of the quenching of AchR intrinsic fluorescence by spin-labeled phospholipids, Chattopadhyay and McNamee (1991) suggested that γ-Trp-453 is positioned at the protein-lipid interface [see also Narayanaswami et al. (1993)]. However γ-Trp-453 was apparently inaccessible to [^{125}I]TID, despite the fact that this residue is positioned equivalently to labeled residues α-Cys-412 and β-Tyr-441. This lack of reaction with [^{125}I]TID, however, does not result from inaccessibility from the lipid phase, because γ-Trp-453 reacts with another hydrophobic probe, [^{3}H]diazofluorene (Blanton et al., 1994). Tyr-441 in β-M4 and Trp-453 in γ-M4 are unique residues in that their location along the α-helix (or along a β-sheet) would allow the hydrophobic portion of the amino acid side chain to be located in the hydrophobic core of the bilayer while the polar portion of the side chain is situated such that it may hydrogen bond with either the carbonyl or the polar head group of an adjacent phospholipid molecule [see Schiffer et al. (1992)].

For the M3 segments the pattern of [^{125}I]TID labeling defines a strip of α-helix in contact with lipid and indicates that the positively charged residues located at the N- and C-termini of each M3 segment face the lipid bilayer. This conclusion contradicts a prediction (Raines & Miller, 1993) that these positively charged side chains would not face lipid, based upon the lack of effect of pH or salt on the number of positively charged lipids at the protein–lipid interface. Our results indicate that the charged side chains at the ends of M3 or M4 segments are oriented toward the lipid, where they

may participate in hydrogen bonding to carbonyl or polar head groups of phospholipids.

The sites of [^{125}I]TID incorporation into α-M1 were determined under three conditions: [−/+], [+/+], and ([+/−]; data not shown). In each of these cases the pattern of ^{125}I release was essentially the same as expected for [^{125}I]TID incorporation into residues situated at the lipid–protein interface of the AchR. [^{125}I]TID was incorporated into Cys-222, Leu-223, Phe-227, and Leu-228. The periodicity of labeled residues is inconsistent with the pattern expected for labeling either of a face of an α-helix or of a β-sheet. What is clear is that the labeling is restricted to the C-terminal half of α-M1 beyond Pro-221. It is noteworthy that Cys-222 is by no means the dominantly labeled amino acid. This result suggests that [^{125}I]TID has only very limited access to at least the side chain of Cys-222 and that Cys-222 may not be located at the protein–lipid interface. One possibility is that the M1 region possesses α-helical secondary structure but that the presence of Pro-221 introduces enough distortion into the helix to allow [^{125}I]TID limited access to a portion of Cys-222.

The [^{125}I]TID sites of labeling in the M1 region of the α-subunit reflect labeling of residues which are situated at the lipid–protein interface of the AchR. These residues are quite removed from the sites of specific labeling by the photoactivatable, noncompetitive inhibitor [^{3}H]quinacrine azide, which are restricted to residues at the extracellular end, Arg-209 and Pro-211 [DiPaola et al., 1990; Karlin, 1991; but see also Arias et al. (1993)]. Previously the [^{125}I]TID sites of incorporation into the M1 region of the δ-subunit were identified as Phe-232, Ile-233, and Cys-236 ([+/−]; White & Cohen, 1992). Interestingly, [^{125}I]TID incorporation into these residues was not observed in the absence of agonist [−/−], and yet the labeling appeared to be consistent with labeling of the AchR from the lipid phase. The results suggest that at least in the case of the δ-M1 region there is an agonist-induced change in the regions of the AchR exposed to the lipid bilayer. In contrast, there does not appear to be any labeling of the M1 region of the β-subunit (White & Cohen, 1992; and unpublished observations), and preliminary results indicate [^{125}I]TID incorporation into Cys-230 and Ser-235 of the M1 region of the γ-subunit [+/+]. Further work will be required to understand both the nature of the secondary structure of the M1 region as well as any possible AchR "state"-dependent changes in the exposure of the M1 region of each subunit to the lipid bilayer.

ACKNOWLEDGMENT

We thank David Chiara for providing valuable assistance in performing N-terminal sequence analysis as well as for his valuable comments and suggestions. We also thank Martin Gallagher for his helpful comments.

REFERENCES

Akabas, M. H., Stauffer, D. A., Xu, M., & Karlin, A. (1992) *Science 258*, 307–310.

Arias, H. R., Valenzuela, C., & Johnson, D. A. (1993) *J. Biol. Chem. 268*, 6348–6355.

Blanton, M. P., & Cohen, J. B. (1992) *Biochemistry 31*, 3738–3750.

Blanton, M. P., Raja, S. K., Lala, A., & Cohen, J. B. (1994) (Abstract submitted to Biophysical Society Meeting).

Bauer, A. W., Oman, C. L., & Margolies, M. N. (1984) *Anal. Biochem. 137*, 134–142.

Changeux, J. P., Galzi, J.-L., Devillers-Thiery, A., & Bertrand, D. (1992) *Q. Rev. Biophys. 25*, 395–432.

Charnet, P., Labarca, C., Leonard, R. J., Vogelaar, N. J., Czyzyk, L., Gouin, A., Davidson, N., & Lester, H. A. (1990) *Neuron 2*, 87–95.

Chattopadhyay, A., & McNamee, M. G. (1991) *Biochemistry 30*, 7159–7164.

Claudio, T., Ballivet, M., Patrick, J., & Heinemann, S. (1983) *Proc. Natl. Acad. Sci. U.S.A. 80*, 1111–1115.

Cleveland, D. W., Fischer, S. G., Kirschner, M. W., & Laemmli, U. K. (1977) *J. Biol. Chem. 252*, 1102–1106.

DiPaola, M., Czajkowski, C., & Karlin, A. (1989) *J. Biol. Chem. 264*, 15457–15463.

DiPaola, M., Kao, P. N., & Karlin, A. (1990) *J. Biol. Chem. 265*, 11017–11029.

Donnelly, D., Overington, J. P., Ruffle, S. V., Nugent, J. H., & Blundell, T. L. (1993) *Protein Sci. 2*, 55–70.

Dreyer, E. B., Hasan, F., Cohen, S. G., & Cohen, J. B. (1986) *J. Biol. Chem. 261*, 13727–13734.

Engelman, D. M., & Zaccai, G. (1980) *Proc. Natl. Acad. Sci U.S.A. 77*, 5894–5898.

Giraudat, J., Montecucco, C., Bisson, R., & Changeux, J. P. (1985) *Biochemistry 24*, 3121–3127.

Giraudat, J., Dennis, M., Heidmann, T., Chang, J., & Changeux, J. P. (1986) *Proc. Natl. Acad. Sci. U.S.A. 83*, 2719–2723.

Giraudat, J., Dennis, M., Heidmann, T., Haumont, P.-Y., Lederer, F., & Changeux, J.-P. (1987) *Biochemistry 26*, 2410–2418.

Hager, D. A., & Burgess, R. R. (1980) *Anal. Biochem. 109*, 76–86.

Hucho, F. (1986) *Eur. J. Biochem. 158*, 211–226.

Imoto, K., Methfessel, C., Sakmann, B., Mishina, M., Mori, Y., Konno, T., Fukuda, K., Kursaki, M., Bujo, H., Fujita, Y., & Numa, S. (1986) *Nature 324*, 670–674.

Imoto, K., Busch, C., Sakmann, B., Mishina, M., Konno, T., Nakai, J., Bujo, H., Mori, Y., Fukuda, K., & Numa, S. (1988) *Nature 335*, 645–648.

Imoto, K., Konno, T., Nakai, J., Wang, F., Mishina, M., & Numa, S. (1991) *FEBS Lett. 289*, 193–200.

Karlin, A. (1991) *Harvey Lect. 85*, 71–107.

Karlin, A. (1993) *Curr. Opin. Neurobiol. 3*, 299–309.

Laemmli, U. K. (1970) *Nature 227*, 680–685.

Leonard, R. J., Labarca, C. G., Charnet, P., Davidson, N., & Lester, H. A. (1988) *Science 242*, 1578–1581.

Li, L., Lee, Y. H., Pappone, P., Palma, A., & McNamee, M. G. (1992) *Biophys. J. 62*, 61–63.

Lowry, O. H., Rosebrough, N. S., Farr, A. L., & Randall, R. J. (1951) *J. Biol. Chem. 193*, 265–275.

Marquez, J., Iriarte, A., & Martinez-Carrion, M. (1989) *Biochemistry 28*, 7433–7439.

McCarthy, M., & Stroud, R. M. (1989) *J. Biol. Chem. 264*, 10911–10916.

Middleton, R. E., & Cohen, J. B. (1991) *Biochemistry 30*, 6987–6997.

Narayanaswami, V., Kim, J., & McNamee, M. G. (1993) *Biochemistry 32*, 12413–12419.

Noda, M., Takahashi, H., Tanabe, T., Toyosato, M., Furutani, Y., Hirose, T., Asai, M., Inayama, S., Miyata, T., & Numa, S. (1982) *Nature 229*, 793–797.

Noda, M., Takahashi, H., Tanabe, T., Toyosata, M., Kikyotani, S., Hirose, T., Asai, M., Takashima, H., Inayama, S., Miyata, T., & Numa, S. (1983a) *Nature 301*, 251–255.

Noda, M., Takahashi, H., Tanabe, T., Toyosata, M., Kikyotani, S., Furutani, Y., Hirose, T., Takashima, H., Inayama, S., Miyata, T., & Numa, S. (1983b) *Nature 302*, 528–532.

Pedersen, S. E., Dreyer, E. B., & Cohen, J. B. (1986) *J. Biol. Chem. 261*, 13735–13743.

Pedersen, S. E., Liu, W.-S., & Cohen, J. B. (1992) *J. Biol. Chem. 267*, 10489–10499.

Popot, J.-L., & Changeux, J. P. (1984) *Physiol. Rev. 64*, 1162–1239.

Raftery, M. A., Hunkapiller, M. W., Stader, C. D., & Hood, L. E. (1980) *Science 208*, 1454–1457.

Raines, E., & Miller, K. (1993) *Biophys. J. 64*, 632–641.

Rees, D. C., DeAntonio, L., & Eisenberg, D. (1989) *Science 245*, 510–513.
Reynolds, J. A., & Karlin, A. (1978) *Biochemistry 17*, 2035–2038.
Schagger, H., & von-Jagow, G. (1987) *Anal. Biochem. 166*, 368–379.
Schiffer, M., Chang, C. H., & Stevens, F. J. (1992) *Protein Eng. 5*, 213–214.
Sigrist, H., Muhlemann, M., & Dolder, M. (1990) *J. Photochem. Photobiol. B 7*, 277–287.
Sobel, A., Weber, M., & Changeux, J. P. (1977) *Eur. J. Biochem. 80*, 215–224.
Stroud, R. M., McCarthy, M. P., & Shuster, M. (1990) *Biochemistry 29*, 11009–11023.
Tobimatsu, T., Fujita, Y., Fukuda, K., Tanaka, K.-I., Mori, Y., Konno, T., Mishina, M., & Numa, S. (1987) *FEBS Lett. 222*, 56–62.
Toyoshima, C., & Unwin, N. (1990) *J. Cell Biol. 111*, 2623–2635.
Unwin, N. (1993) *J. Mol. Biol. 229*, 1101–1124.
Villarroel, A., & Sakmann, B. (1992) *Biophys. J. 62*, 196–205.
Villarroel, A., Herlitze, S., Koenen, M., & Sakmann, B. (1991) *Proc. R. Soc. London B 243*, 69–74.
von Heijne, G. (1986) *EMBO J. 5*, 3021–3027.
von Heijne, G. (1991) *J. Mol. Biol. 218*, 499–503.
White, B. H. (1991) Characterization of the Nicotinic Acetylcholine Receptor, Ph.D. Dissertation, Washington University School of Medicine, St. Louis, MO.
White, B. H., & Cohen, J. B. (1988) *Biochemistry 27*, 8741–8751.
White, B. H., & Cohen, J. B. (1992) *J. Biol. Chem. 267*, 15770–15783.
White, B. H., Howard, S., Cohen, S. G., & Cohen, J. B. (1991) *J. Biol. Chem. 266*, 21595–21607.
Yeates, T. O., Komiya, H., Rees, D. C., Allen, J. P., & Feher, G. (1987) *Proc. Natl. Acad. Sci. U.S.A. 84*, 6438–6442.